Physics – Uspekhi **48** (7) 733 – 742 (2005)

INSTRUMENTS AND METHODS OF INVESTIGATION PACS numbers: **47.40.–x, 62.50.+p**, 82.20.Wt, **96.35.–j**, 96.50.Gn

Deep Impact experiment: possible observable effects

B A Klumov, V V Kim, I V Lomonosov, V G Sultanov, A V Shutov, V E Fortov

DOI: 10.1070/PU2005v048n07ABEH004489

Contents

Abstract. A hypervelocity collision of a metal impactor and the nucleus of the Tempel 1 comet is to be carried out in July 2005 in the framework of the Deep Impact active experiment in space. This paper discusses certain observable consequences of this impact. Numerical simulation of the impact process made it possible to evaluate the diameter of the impact-produced crater as a function of the initial density and porosity of the cometary nucleus. A substantial part of the shockwave-compressed cometary material that is evaporated at the unloading stage may become heated to temperatures on the order of $(1-2) \times 10^4$ K. A change in the chemical composition of the hot vapor in the process of its expansion was computed using a model elemental composition of the cometary nucleus; this may prove useful for determining the parameters of the flash induced by the impact in the visible optical, UV, IR, and radio wavelength bands.

1. Introduction

The study of comets occupies an important place in the study of the evolution of the solar system. One of the reasons for this is that we expect comets to contain the primordial material of the gas-dust protoplanetary cloud from which our solar system evolved about 4.5 billion years ago. How comets formed, that is, how such kilometer-size cosmic bodies were formed as a result of the aggregation of meter- and less-than-a-meter bodies is one of the key problems, not yet resolved, of planetary cosmogony. It is typically assumed that comets were formed at extremely low temperatures, under conditions of slow collisions of sub-meter fluffy bodies [consisting of frozen volatile compounds (H_2O, CO, CO_2, etc) and also of dust particles, mostly of silicates]. This process was followed by their aggregation at later stages. It is commonly considered, therefore, that the chemical and isotropic composition of cometary nuclei may reveal information about the conditions under which comets were formed, that is, information on the state of the early solar system long before their formation (see, e.g., Ref. [1]).

B A Klumov Max Planck Institute for Extraterrestrial Physics, Postfach 1312, Giessenbachstrasse 85748, Garching 85741, Germany
Tel. (49 89) 30000-33-96. Fax (49 89) 3000-35-69
E-mail: klumov@mpe.mpg.de
V V Kim, I V Lomonosov, V G Sultanov, A V Shutov Institute for Chemical Physics Problems, Russian Academy of Sciences, prosp. Akademika N N Semenova 1, 142432 Chernogolovka, Moscow Region, Russian Federation
Tel./Fax (7-095) 785 70 29
E-mail: kim@ficp.ac.ru, ivl143@ficp.ac.ru, sultan@ficp.ac.ru, shutov@ficp.ac.ru
V E Fortov Institute for High Energy Density, Russian Academy of Sciences, ul. Izhorskaya 13/19, 127412 Moscow, Russian Federation
Tel. (7-095) 484 23 00, (7-095) 483 23 14. Fax (7-095) 485 79 90
E-mail: fortov@ras.ru, fortov@ihed.ras.ru

Received 7 June 2005
Uspekhi Fizicheskikh Nauk **175** (7) 767 – 777 (2005)
Translated by V I Kisin; edited by M S Aksent'eva

2. Study of comets

Considerable progress has been achieved in cometary research in recent years. Among the first successful projects we can list the missions of automatic interplanetary stations Vega-1 and Vega-2 to the Halley comet in 1986 [2]. More than one and a half thousand photographs of the comet from different distances $(8-14{,}000) \times 10^3$ km were obtained, the reflectivity of the surface of the cometary nucleus was determined, the chemical composition of nearly 2000 particles of cometary origin was analyzed using a mass spectrometer, and the amount of material ejected from the nucleus was evaluated as $5-10$ t s^{-1}.

The destruction of the Shoemaker-Levy 9 (SL9) comet by tidal forces not long before a comet collided with Jupiter in 1994 (see, e.g., Ref. [3]) demonstrated that comets have low tensile strength ($\sim 10^3$ dyn cm^{-2}), at least on scales on the order of 1 km; this is an indication of the low density and high porosity of the cometary nucleus [4], thus supporting the popular model of the cometary nucleus as a conglomeration of rocky bodies bound together by ice (the rubble pile model) [5]. Observations of the Halle – Bopp and Hyakutake comets in the mid-1990s provided important information on the chemical and isotopic composition of the gas and dust components of the coma and, hence, on the composition of volatile compounds in the cometary nucleus. However, a

Figure 1. Photograph of the surface of the Wild 2 comet obtained by the space probe Stardust [5]. As matters stand, this photograph was made from a record short distance of $\simeq 250$ km. Numerous clearly pronounced craters are traces of bombardment of the surface of the nucleus. (Image credit: NASA, Jet Propulsion Laboratory.)

breakthrough in our understanding of the origin and evolution of comets is mostly anticipated from comet missions that send a specialized probe to a selected comet in order to study the properties of the comet from a short distance. Several such probes have been launched in recent years.

The return of the space mission Stardust, launched in February 1999, carrying back specimens of dust particles from the coma of the comet Wild 2 is expected at the beginning of 2006. Stardust closed in on Wild 2 to a record distance of ≈ 250 km and sent home what are currently the most detailed photographs of the surface of a comet [6]. Figure 1 displays one of these unique photographs of the surface of Wild 2. It is clearly seen that the surface is covered by numerous craters and resembles the surface of a rocky asteroid, which presumably points to the absence of volatile compounds in the surface layer of the comet's nucleus.

According to plans, the Rosetta mission (launched in 2004, expected to return in 2015) will study in detail the nucleus of the 67P/Churumov – Gerasimenko comet and will deliver to the Earth a sample of the cometary material extracted from a depth of ≈ 1 m. The mission is to obtain very important (currently unavailable) information on the density of the comet's nucleus. [1]

[1] Along with a discussion of successful cometary missions, we need to mention that contact was lost in the last several years with two cometary probes, CONTOUR and Deep Space 1. The Comet Nucleus Tour (CONTOUR) mission was launched in June 2002; radio contact was lost six weeks later. The mission was expected to approach three comets (Encke, Schwassmann – Wachmann-3, and d'Arrest) and to conduct a detailed study of the coma's composition, as well as a study at a distance of the surface properties of the nuclei of these three comets. The space probe Deep Space 1 (launched in October 1998, lost in 2001) fulfilled its main (technological) task and also obtained high-resolution photographs of the 19P/Borelly comet.

Note that the surface layer of the cometary material accessible for study may be substantially modified by cosmic rays, solar radiation, and micrometeorite bombardment.

Absorption of solar radiation results in evaporation of volatile components and therefore in a drop in their concentration in the surface layers of a comet's nucleus. Penetrating radiation (including charged-particle irradiation) is capable of modifying the surface layer of the nucleus to a depth $l_{\rm m}$ equal within an order of magnitude to the radiation's free path [2], i.e., $l_{\rm m} \sim 1-10$ cm.

In the case of a micrometeorite-induced transformation of the surface of a comet's nucleus, $l_{\rm m}$ may be considerably longer. The characteristic thickness of the modified layer may be found by analogy to [7], which evaluated, among other parameters, the rate of transformation of lunar ice in cold traps. Assuming constant micrometeorite flux, we can find an estimate of the depth of the modified layer for a comet's nucleus: over the characteristic time of a comet's existence ($\sim 3 \times 10^9$ years), impacts of micrometeorites reprocess the surface layer of the comet's nucleus to a depth of $l_{\rm m,\,m} \sim 3$ m. It is assumed that the transformed material is not ejected from the nucleus. This is not always correct: for instance, high impact velocities result in erosion, that is, rather in the removal of cometary material than in its modification, and this in fact gives the upper bound as $l_{\rm m,\,m} \leqslant 3$ m.

An analysis of a coma's optical emission can provide certain information on the composition of volatile compounds in the surface (modified) layer. No data is available on the composition of deeper layers of comets' nuclei. It is therefore very important to establish what differences exist between the compositions of the surface (modified) and deeper layers of a comet nucleus.

We expect from the Rosetta mission that the Rosetta Lender dropped to the surface of the comet will extract a sample of material from a depth of approximately 1 m. If $l_{\rm m} > 1$ m, the sample would have come from a modified layer, which probably would not allow us to identify the composition of the primeval material of a protoplanetary cloud. Such information can be obtained by the Deep Impact active experiment [8 – 12].

3. Deep Impact: active experiment in space

The Deep Impact project is to study a hypervelocity collision of a metal impactor with the nucleus of the comet 9P/Tempel 1. It is expected that this collision will excavate a crater with characteristic size $S_{\rm c} \simeq 100$ m and a depth $D_{\rm c} \simeq 30$ m $\gg l_{\rm m,\,m}$ that can be investigated by optical techniques. The observation of the crater formation process during collision may provide indirect information on the density and strength of the nucleus. It is also anticipated that this impact will generate an active zone on the surface of the comet's nucleus, triggering a prolonged period of intense emission of volatile compounds. The fluorescence of these volatile compounds excited by solar radiation will also be observed by instruments onboard the Deep Impact probe. The Deep Impact mission was launched in January 2005 and the collision of its impactor with the comet Tempel 1 is expected on July 4, 2005.

The short-revolution-period comet Tempel 1 is currently revolving with a period of 5.5 years with a perihelion of

[2] We do not consider here the modification caused to comets' nuclei by the interaction with cosmic rays since they affect the bulk of the nucleus.

1.5 a.u. and aphelion of 4.8 a.u. At the moment of collision the comet will be lying at its perihelion at a distance of 0.89 a.u. from the earth and approximately 1.5 a.u. from the sun. The choice of this comet was dictated by the temporal restrictions on the project and by reasons of navigation; to these were added the requirements of hypervelocity intersection of the orbits of the impactor and the target at a moment of time that would be convenient for observation from the earth, plus a number of requirements relating to the comet's properties: the short period of revolution around the nucleus's axis, the relatively large size of the nucleus ($\simeq 6$ km), and some others.

At the moment of the collision of the impactor and the comet's nucleus, the Deep Impact flyby spacecraft will be approximately 500–700 km away from Tempel 1, making it possible to observe the processes induced by the collision at high resolution. Numerous land-based observatories and the Hubble Space telescope on its orbit will also observe the impact.

We will now list here the parameters of the Deep Impact experiment. The copper impactor shaped into a spherical segment with navigation equipment has a mass $m_i \simeq 370$ kg, diameter $d_i \simeq 1$ m, height $h_i \simeq 1$ m; it will collide with the nucleus of the comet Tempel 1 at a velocity $v_i \approx 10.2$ km s^{-1} [8]. The expected density of the comet's nucleus is $\rho_c \sim 0.3$–1.5 g cm^{-3}. The recording system includes telescopes to record images using CCD matrices with a resolution of 1.4–7 m/pixel and a multifunctional visible light spectrometer and an infrared spectrometer for the 1.05–4.8 μm range with a resolution $\lambda/\Delta\lambda \geqslant 216$ [9]. We need to emphasize that such parameters of the comet's nucleus as, for example, density, porosity, and chemical composition, which considerably affect the process, are unknown and also constitute a subject of investigation for the Deep Impact mission.

Let us look at the process of impact in more detail. This process has a number of specific features that characterize the occurring physicochemical states of matter. Note that at a velocity $v_i = 10.2$ km s^{-1} the impactor material (copper) remains solid on impact, so that the dynamics of impact processes will mostly involve the cometary matter. The impact generates a shock wave (SW) in the target and as it propagates through the cometary material, the unloading wave forms. This process creates a broad spectrum of phase states: from a compressed hot liquid at the shock wave front to a low-density and evaporated liquid in which various chemical reactions take place, to fractured solid material at the late stages of post-explosion expansion. Furthermore, the gravitational field of the relatively small nucleus can be neglected, that is, we assume that practically the entire material evaporated and destroyed by the collision is ejected from the comet.[3]

The shape and size of the crater depend essentially on the initial density of the cometary material. Experiments show that an impact with a low-density nucleus will produce not a crater that can be described by relatively simple similarity laws, but a cavity, often of complex shape, that does not yield to description by simple scaling [13, 14]. Moreover, a considerable part of the impactor's energy is consumed in a low-density target as work on pore collapse and goes into increasing the internal energy, entropy, and temperature of the cometary material. The shock wave amplitude is then lower, and its damping is considerably faster, while the finite states in the unloading wave have higher temperatures as compared to the case of collision with a higher-density target.

A comet possesses its own atmosphere, with the concentration of particles N_c at the surface of the nucleus on the order of $N_c \sim L_s N_A/(4\pi r_{sc}^2 Q_{v,w}\mu_w) \sim 10^{13}-10^{14}$ cm^{-3}, where L_s is the sun's luminosity, r_{sc} is the distance from the comet or the sun at the moment of impact ($r_{sc} \simeq 1.5$ a.u.), $Q_{v,w}$ is the evaporation heat of the comet ice (the estimate was obtained for water ice), μ_w is the molar mass of water, and N_A is Avogadro's number. Since the particle concentration in the coma in the neighborhood of the nucleus decreases with distance as $N_c \propto (r_c/r)^{-2}$, where r_c is the radius of the comet (for Tempel 1, $r_c \simeq 3$ km), we immediately conclude that the impactor undergoes practically no braking in the cometary atmosphere: the corresponding braking efficiency factor is $N_c\mu_w r_c \pi d_i^2/(4N_A m_i) \simeq 10^{-5} \ll 1$.

The mass of the evaporated ejecta m_v can be evaluated by using a relation [15, 16] between the mass of the shock-generated vapor and the impact parameters; this relation is based on numerical simulation of impact processes:

$$m_v \simeq m_i \left\{ 2\left[\frac{4}{v_i}\left(\frac{Q_v}{v}\right)^{0.5}\right]^{v-2} - 1 \right\}. \quad (1)$$

Here, m_i is the impactor mass and v is a numerical coefficient (in continuous media, $v \simeq 0.33$ [16]). For the impact parameters in the case in question, $m_v \simeq 0{,}7 m_i \simeq 250$ kg.

Note that the above quantity can be evaluated using a different approach. Depending on the distance z to the impact point, the damping of pressure p at the SW front can be found from the relation

$$p \propto \left(\frac{z}{L}\right)^{-\eta}, \quad (2)$$

where L is the characteristic scale of SW damping in the target and η is the effective exponent of the adiabat (typically $\eta \simeq 2.5-3$). To calculate L, a formula of the following type is often used (see, e.g., Ref. [15]): $L = d_i(\rho_i/\rho_t)^{\alpha}(v_i/c_s)^{\beta}$, where d_i is the impactor size, ρ_i is the impactor density, ρ_t is the target density (in our case it is the comet's nucleus density ρ_c), v_i and c_s are the impactor velocity and the speed of sound in the target material, and α and β are constants that depend on the target material. For instance, for hypervelocity impact on water, $L = L_w \simeq (2-3)d_i$ [17].

After the SW front has passed, the material of the target acquires specific energy e; it can be shown, using the equation of state of water [18], that in the impact zone ($z \leqslant L$) $e \simeq v_i^2$. When the load on the shock-compressed comet material is relieved, it begins to evaporate and if $e \gg Q_v$ then all of it evaporates. Since a SW damps out over a distance $z \simeq L_w$ from the impact location, the mass of the evaporated matter can be found as $m_v \sim \rho_t d_i^2 L_w \sim m_i \sim 200$ kg, which is in good agreement with the estimate obtained earlier. The initial vapor temperature is $T_0 \lesssim v_i^2/2c_v$, where c_v is the heat capacity of water. This gives us an estimate of the upper bound on T_0: $T_0 \lesssim 10^4$ K. More accurate values for the above quantities can be obtained by numerical simulation of the impact process.

The purpose of the present paper is to evaluate the observable effects of the Deep Impact active experiment on the basis of a number of model computations of the impact process. Among these, we count the size of the generated crater, the formation of the hot cloud of material evaporated

[3] The escape velocity for the comet Tempel 1, $v_{esc} \sim 1$ m s^{-1}, is much lower than the characteristic velocities acquired by the destroyed cometary material in the unloading wave.

from the cometary nucleus at the unloading stage in the shock-compressed layers, optical emission from this cloud, etc.

4. Numerical simulation of the impactor-target collision in the Deep Impact experiment

Water ice of different porosity was chosen as a material of the cometary nucleus (the target) to simulate the process of a hypervelocity impactor-target collision. According to thermodynamical calculations, various physicochemical processes occur in the impactor and target materials at the impact velocity $v_i = 10.2$ km s^{-1}, in particular, irreversible heating at the front of the generated shockwave with pressure reaching 110 GPa. This pressure results in the melting and subsequent evaporation of cometary material during the expansion of the ejecta curtain. To describe the collision process, a set of gas dynamics equations was solved numerically,

$$\frac{\partial\rho}{\partial t} + \operatorname{div}\rho\mathbf{u} = 0\,, \tag{3}$$

$$\frac{\partial\rho\mathbf{u}}{\partial t} + \operatorname{div}(\rho\mathbf{u}\times\mathbf{u} + \pi) = 0\,, \tag{4}$$

$$\frac{\partial\rho(E+u^2/2)}{\partial t} + \operatorname{div}\left[\rho\mathbf{u}\left(E+\frac{u^2}{2}\right) + \pi\mathbf{u}\right] = 0\,, \tag{5}$$

where $\partial/\partial t$ is the local (i.e., taken at a given point in space) partial derivative with respect to time, ρ is the matter density, $\mathbf{u} = (u_x, u_y, u_z)$ is the velocity vector, $\pi = \|\pi_{ik}\|$ is the stress tensor[4], and V is an arbitrary volume of three-dimensional space. Equations (3)–(5) are the expression for the laws of conservation of mass, momentum, and energy. The set (3)–(5) was closed by using the equations of state for the impactor and target materials and was solved numerically. We used a moving mesh hydrocode of second order of accuracy in space; the code resolves the shock front quite well [19].

This paper uses the broad-range multiphase equation of state (EOS) in copper [18]. The model equation of state is given as a thermodynamically complete free energy potential and takes into account the contributions of the ion and electron subsystems, as well as the high-temperature effects of melting, evaporation, and ionization. When constructing the EOS we used the data of a stationary thermophysical experiment, those of compressibility measurements with diamond anvils, the data on the electroexplosion of conducting wires, the results of dynamic experiments on shock compression and isentropic expansion of balk and porous specimens, and also computations based on the Thomas–Fermi and Debye–Hückel theories. On the basis of this model, an EOS was developed of the high-pressure phase of the ice-VI phase that corresponds to the range of the phase diagram that the Deep Impact experiment can produce. The quality of the EOS used in this work is illustrated in Fig. 2 where the computed energy surface in copper is shown.

The initial stage of the collision is shown in Figs 3 and 4. For simplification, the process of the *vertical* fall of a copper impactor on a flat surface of a comet's nucleus whose model composition is identical to the composition of water ice of various porosity Po ($Po = 1 - V_0/V$, where V_0, V are the specific volumes of pores and of cometary material, respectively) was studied. With this impact geometry, the observable effects of the collision will be especially well pronounced. Two cases were considered: $Po = 1$ (non-porous ice) and $Po \simeq 0.5$, which cover part of the range of possible variations of the cometary nucleus's density.

[4] Note that the stress tensor is spherical in the hydrodynamic approximation: $\pi_{ik} = P\delta_{ik}$, δ_{ik} is the Kronecker symbol.

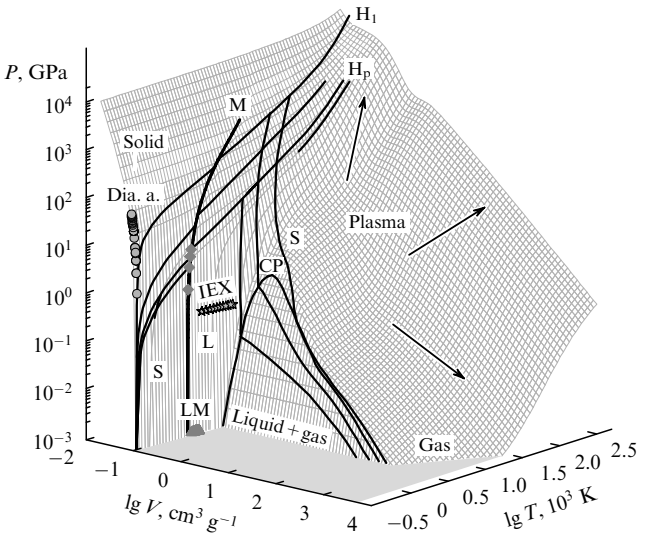

Figure 2. 3D surface of pressure-specific volume-temperature in copper. The zones of the aggregate states of matter are shown. Notation: Dia.a. — diamond anvils; LM — the measured density of liquid metal at normal pressure; EEW — data on the expansion of metal into inert gas under pressure (electroexplosion of wires); H_1, H_p — the basic shock adiabat and adiabats of porous specimens; S — expansion isoentropes in shock-compressed copper (calculated shock adiabats and unloading isoentropes correspond to actual experiments); CP — critical point. Arrows indicate the direction of decreasing non-ideality of the system.

Figure 3 represents the density field at different moments of time. Version (a) corresponds to ice of initial density $\rho_0 = 1.35$ g cm^{-3} and porosity $Po = 1$. Version (b) corresponds to porous ice of initial density $\rho_0 \simeq 0.7$ g cm^{-3} and porosity $Po \simeq 0.5$. In both cases the impactor velocity is $v_i = 10.2$ km s^{-1}. The three chosen frames demonstrate the evolution of density both in the impactor and in the target over time (time increases from top to bottom): $t_1 = 0.03$ ms, $t_2 = 0.1$ ms, and $t_3 = 0.3$ ms, respectively.

Note that the expansion velocity of impact-induced gas increases appreciably with decreasing density (and hence with increasing porosity) of the target material. The reason for this is a higher initial temperature of shock-evaporated cloud expanding from higher-porosity water ice. This effect can be reliably detected in view of the fact that observations with a resolution of about 1 m are expected (this high resolution is feasible for the instruments on board the Deep Impact mission). We conclude that model computations indicate that the evolution of the gas ejecta will indirectly provide important information on the density of the cometary nucleus.

Figure 4 represents the temperature field at the indicated moments of time for the same parameters of the impactor and the target. In both cases unloading of the shock-compressed target material generates a cloud of hot gas with a temperature $T \sim 3000$ K; a cumulative rise in temperature on the symmetry axis is observed. The factor causing this increase in temperature lies in collisions of the expanding jets of hot vapor that form in the process of unloading and flow around

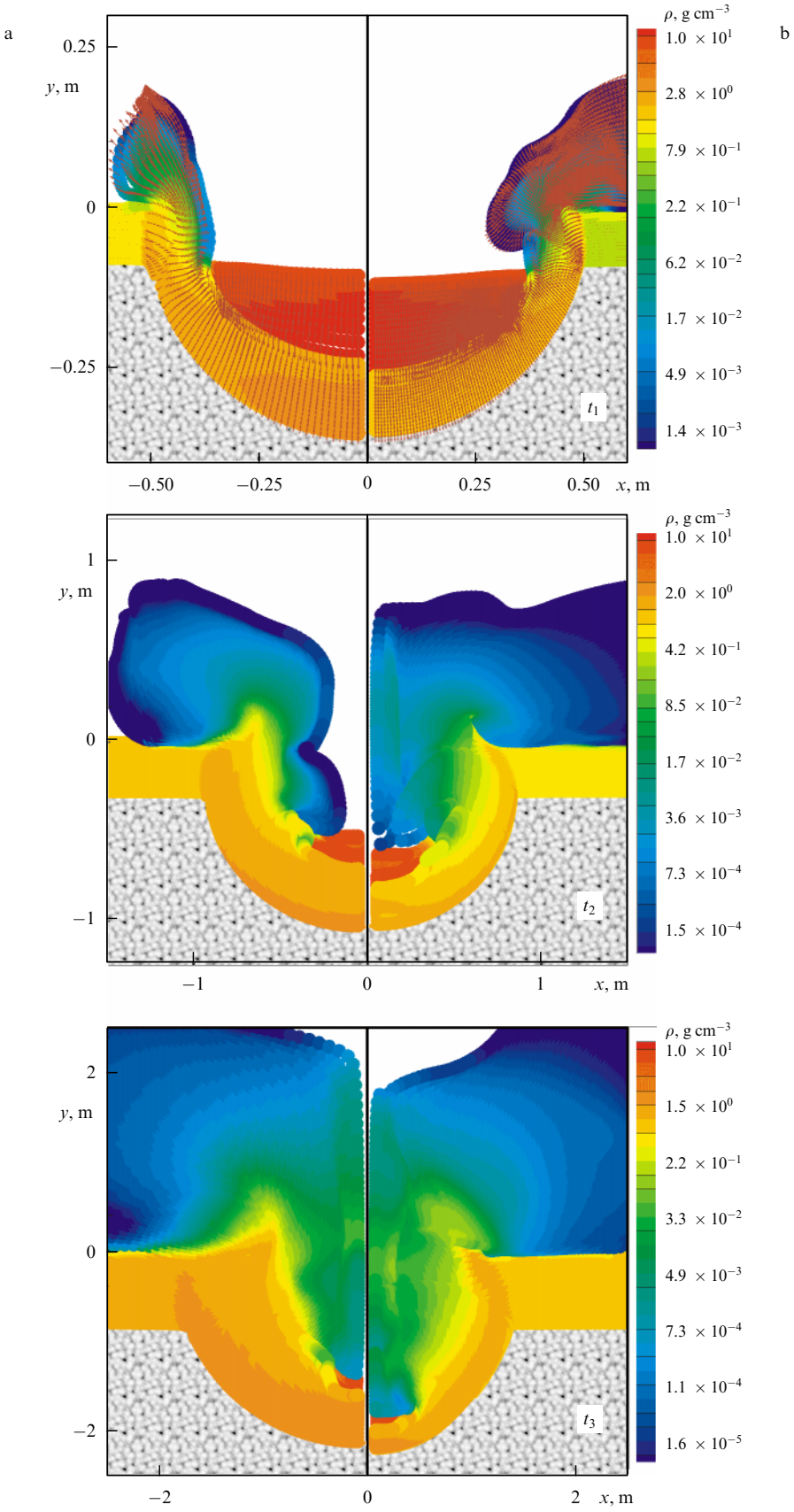

Figure 3. Density field in a hypervelocity collision of a copper impactor with the nucleus of a comet at different moments of time. The data represent a vertical collision, for two versions of target material: version (a) corresponds to ice of initial density $\rho_0 = 1.35$ g cm^{-3}, and version (b) corresponds to porous ice of initial density $\rho_0 \approx 0.75$ g cm^{-3}. In both cases the collision velocity is $v_i = 10.2$ km s^{-1}. The successive frames correspond to time moments (time increases from top to bottom): $t_1 = 0.03$ ms, $t_2 = 0.1$ ms, and $t_3 = 0.3$ ms, respectively.

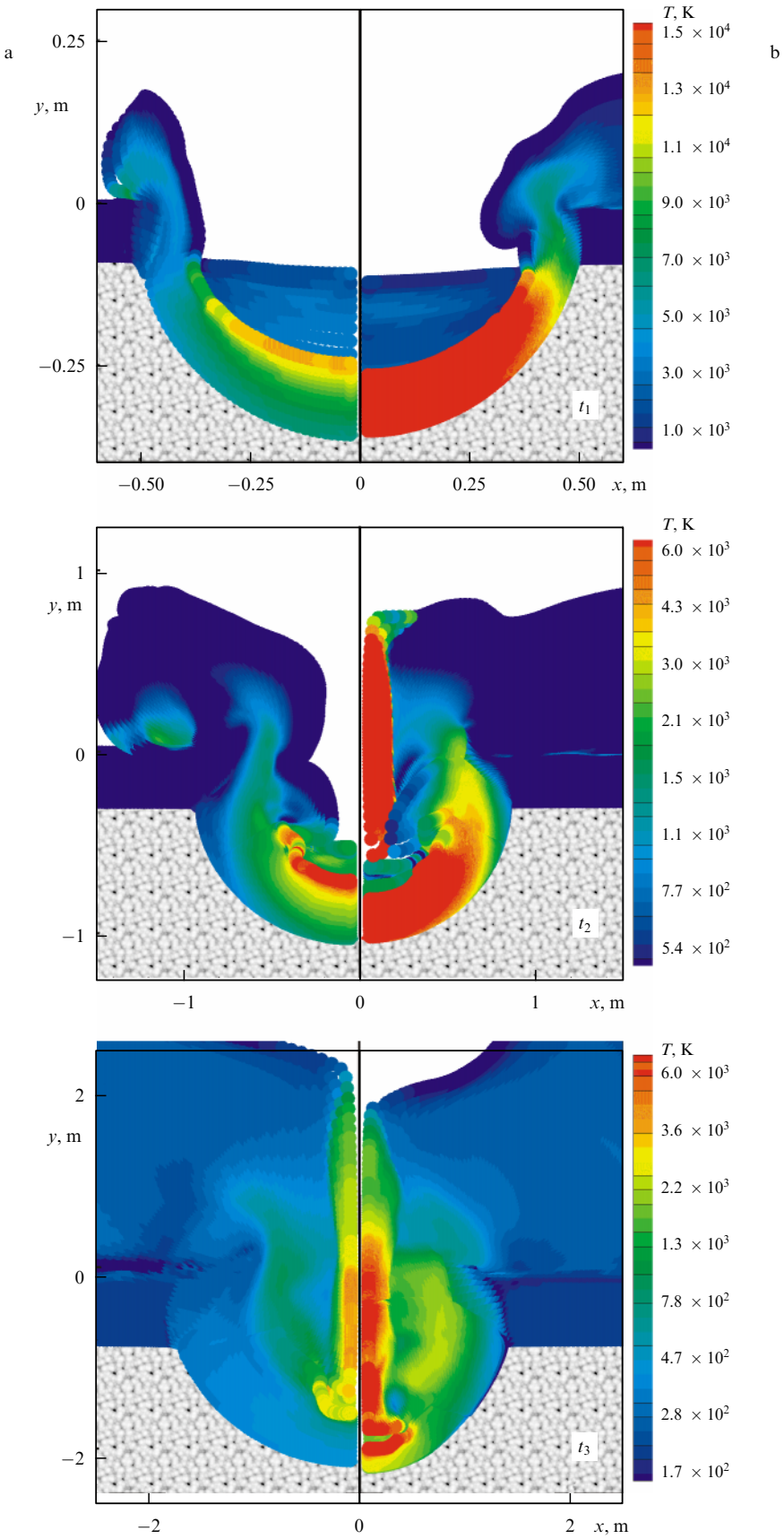

Figure 4. Temperature field in a hypervelocity collision of a copper impactor with the nucleus of a comet at different moments of time. The data represent a vertical collision, for two versions of target material: version (a) corresponds to ice of initial density $\rho_0 = 1.35$ g cm^{-3}, and version (b) corresponds to porous ice of initial density $\rho_0 \approx 0.75$ g cm^{-3}. In both cases the collision velocity is $v_i = 10.2$ km s^{-1}. The successive frames correspond to time moments (time increases from top to bottom): $t_1 = 0.03$ ms, $t_2 = 0.1$ ms, and $t_3 = 0.3$ ms, respectively. In both cases the evaporated cometary material may be heated at the unloading stage to high temperatures: $T_m \simeq 15{,}000$ K for version (a), and $T_m \simeq 35{,}000$ K for version (b).

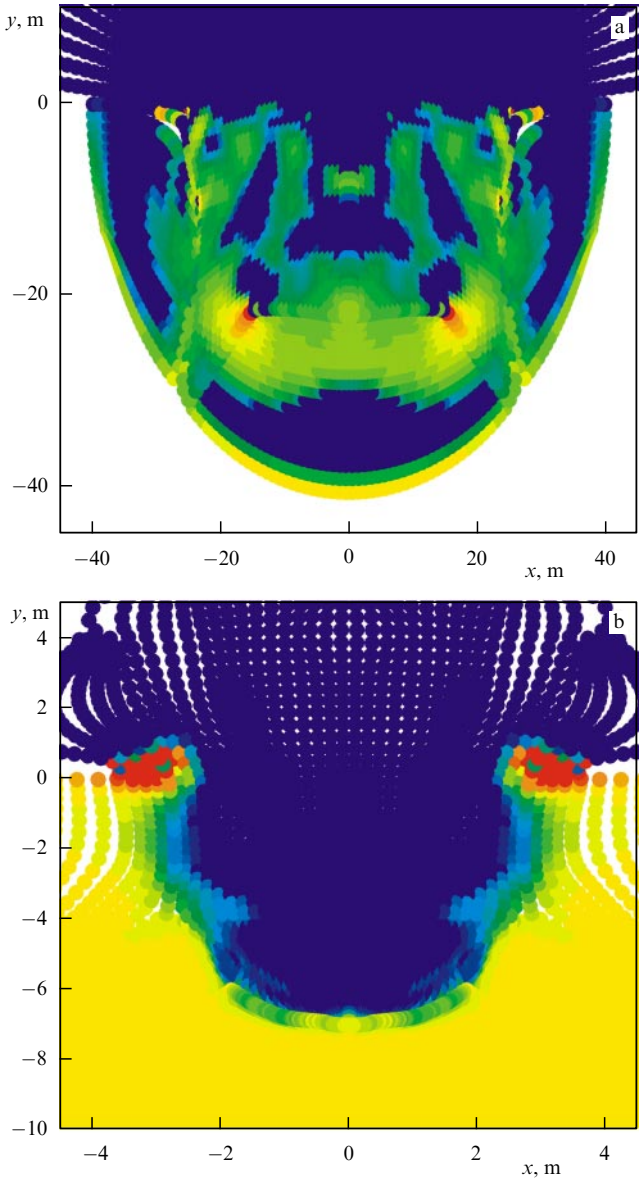

Figure 5. Pressure field in a hypervelocity collision of a copper impactor with the nucleus of a comet at the final stage of crater formation. The data represent a vertical collision, for two versions of target material: version (a) corresponds to ice of initial density $\rho_0 = 1.35$ g cm^{-3}, and version (b) corresponds to porous ice of initial density $\rho_0 \approx 0.75$ g cm^{-3}. In both cases the collision velocity is $v_i = 10.2$ km s^{-1}. In case (a) the crater is of diameter $S_c \simeq 80$ m and depth $D_c \simeq 40$ m. In case (b) the crater is much smaller: $S_c \simeq 5$ m, and its depth is $D_c \simeq 6$ m.

the impactor. In the case of porous ice, the maximum temperature induced by the impact of vapor may be quite high — $T_{m,\,p_0} \simeq 25{,}000$ K, which is considerably higher than the maximum temperature in the cloud of vapor formed by an impact on non-porous ice ($T_{m,\,ice} \simeq 15{,}000$ K). We discussed the cause of this effect of greater heating of porous matter above.

Figure 5 shows the pressure field at the final stage of crater formation in non-porous ice (a) and in porous ice (b). The shape and size of the resulting crater can be evaluated from the condition that the compressive yield point of ice is $\sigma \simeq 500$ atm. In this case, if we neglect the gravitational field of the comet, the entire material exposed to shock compression above this limit should be fractured and thrown off the comet in the unloading wave (the ejection velocity of the cometary material under isentropic unloading from a pressure of ≈ 500 atm equals approximately 15 m s^{-1}, which is much greater than the escape velocity for this comet).

Figure 5 shows quite clearly the zones separating the destroyed and intact ice; correspondingly, the parameters of the crater can be estimated. For non-porous ice the crater depth is $\simeq 40$ m, and its diameter $\simeq 80$ m. Such craters will be readily observable from the Deep Impact flyby spacecraft. In the case of porous ice, the crater size is considerably smaller: the crater depth is about 7.5 m and its diameter is 7 m.

This great difference between crater dimensions in the above two versions of target porosity follows from the different physical processes that are responsible for crater formation. In the case of a non-porous ice, the impactor generates a strong shock wave moving far ahead of the impactor, so the crater size is determined by the material transported in the unloading wave. In the case of porous ice the shock wave fails to advance far ahead of the impactor and the main fraction of energy is consumed by pore collapses, transforming into the internal energy of matter. The shape of the crater is then elongated in the direction of motion of the impactor, with small transverse dimensions. Note that the depth of impactor penetration in non-porous target material is $\simeq 2.5$ m, while in porous material it is much larger: $\simeq 6$ m. Therefore, the transfer dimensions of the crater make it possible to indirectly determine the density of the cometary nucleus.

5. Chemical transformations in the expanding shock-induced vapor cloud

The vertical hypervelocity impact on the nucleus of a comet thus results in the formation of a relatively dense (at density $\rho_{cl} \sim 10^{-2}$ g cm^{-3}) hot gas cloud of characteristic size about 1 m and consisting of shock-evaporated material of the target at a temperature of $T \sim (3-10) \times 10^3$ K. It can be easily shown that this cloud is in thermodynamic equilibrium. We assume that the elemental composition of the hot vapor corresponds to the composition of the coma of a synthetic (model) comet obtained by observing the Halley, Halle–Bopp, and Hyakutake comets [20]. Then the share by volume of elements in the cometary matter is: hydrogen — [H] $\simeq 0.6$, oxygen — [O] $\simeq 0.3$, carbon — [C] $\simeq 0.1$, nitrogen — [N] $\simeq 0.01$, and sulfur — [S] $\simeq 0.003$.

Figure 6 plots the thermodynamically equilibrium chemical composition of the hot gas as a function of its temperature for a prescribed elemental composition for different pressures p ($p = 1$ atm, the inset shows the composition at $p = 10$ atm), covering a broad range of possible initial states of shock-vaporized cometary material. As could be expected, at high temperatures all molecular compounds undergo practically total dissociation and the composition of the hot gas is dominated by atoms of the known elemental composition. The curves plotted in Fig. 6 make it possible to evaluate the initial concentrations of various compounds in the hot cloud. We find that the main compounds in the shock-evaporated cometary material are (fractions by volume are shown): [H] $\simeq 0.6$, [O] $\simeq 0.2$, [OH] $\simeq 0.02$, [CO] $\simeq 0.1$, [N_2] $\simeq 0.003$, [N] $\simeq 0.003$, [NO] $\simeq 0.002$, and [S] $\simeq 0.003$. It is important and interesting from the observational point of view how the chemical composition of this cloud changes while the ejecta fly out. Indeed, many compounds found in the shock-evaporated cometary matter are efficient emitters. We

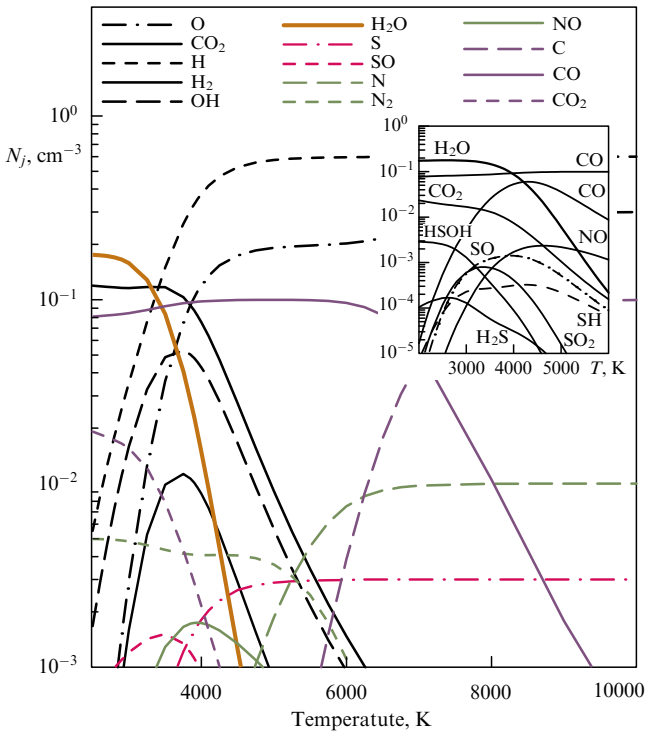

Figure 6. Thermodynamically equilibrium chemical composition of the hot gas as a function of temperature, with the elemental composition of the gas fixed (H:O:C:N:S = 60:30:10:1:0.3). Gas pressure: 1 atm. The inset gives the equilibrium composition of the gas of the same elemental composition but at a pressure of 10 atm. These versions cover a broad range of possible initial states in the shock-evaporated model cometary material.

assume for simplicity that the gas cloud expands by inertia, that is, that the cloud size $d_{\rm cl}$ over the time interval t of interest to us now increases linearly with time: $d_{\rm cl} \sim c_{\rm s,\,cl}\,t$, where $c_{\rm s,\,cl}$ is the speed of sound in hot gas.

Chemical reactions are highly efficient in the hot gas, so its chemical composition may change significantly while the cloud expands. Both density and temperature of the initially hot cloud fall off with time, the rate of chemical reactions diminishes, and the characteristic time of chemical relaxation (time for thermodynamical equilibrium to set in) increases. Obviously, the characteristic time for reaching the equilibrium chemical composition increases in the binary collisions mode as the gas density falls off as $\tau_{\rm ch,\,s} \sim \rho^{-1}$. For three-body collisions it grows as $\tau_{\rm ch,\,t} \sim \rho^{-2}$, and beginning with a certain moment of time $\tau_{\rm q}$ these times exceed the characteristic time $\tau_{\rm hd}$ of gas-dynamic processes that are responsible for the changes in gas temperature and density. It is possible to evaluate $\tau_{\rm hd}$ by the order of magnitude from $\tau_{\rm hd} \sim d_{\rm cl}/c_{\rm s,\,cl}$, where $d_{\rm cl}$ is the size of the vapor cloud and $c_{\rm s,\,cl}$ is the speed of sound in the hot vapor. From this moment on, the composition of the shock-evaporated material remains practically unchanged — the quenching of chemical compounds occurs (see, e.g., Ref. [21]). Note that quenching parameters (pressure and temperature) may be appreciably different for different compounds, so that kinetic calculations have to be conducted for a quantitative determination of the concentrations of quenched compounds.

Spectroscopic observations of the cometary material ejected on impact are planned both for the Deep Impact spacecraft and for ground-based telescopes. It is expected that both the optical emission of the expanding gas and its fluorescence excited by solar light will provide information on the chemical composition of the cometary matter.

Let us find how the chemical composition of the shock-evaporated cometary material changes in the course of expansion. To achieve this, equations of chemical kinetics that describe chemical transformations in shock vapor were solved simultaneously with gas dynamics equations that describe the expansion of the vapor cloud. Approximately 400 gas phase reactions were taken into consideration; these occur at high temperatures in a mixture of H–O–C–N–S-containing compounds and describe the evolution of 40 compounds that comprise the composition of the model shock vapor [22]. Note that the presence of dust in the vapor cloud may greatly modify its chemical composition. This occurs because heterogeneous reactions (involving dust) are typically highly efficient and are capable of greatly accelerating chemical transformations (the particles of dust may act as catalysts). The equations we use do not cover the dust component of shock vapor. The appropriate equations of chemical kinetics are

$$\frac{\partial n_j}{\partial t} = P_j - n_j L_j + n_j \frac{\partial}{\partial t} \ln \rho\,, \qquad (6)$$

where n_j is the average (over the volume of the cloud) concentration of the jth compound, and P_j and L_j describe the sources and losses of the jth compound in chemical reactions (including photoprocesses induced by solar radiation). The last term describes the effect of the expansion of the hot cloud on photochemical processes.

For the initial data for this set of equations, thermodynamically equilibrium values of that concentration were used for the compounds in question, which is justifiable if we take into account the high initial temperatures ($T_0 \sim 6000$ K) and density ($\rho_0 \sim 10^{-2}$ g cm^{-3}) of the vapor cloud.[5]

Figure 7 shows the characteristic time dependences for a number of compounds that are important from the standpoint of observations. Two versions are shown, for different initial temperatures T_0 of the hot vapor cloud: $T_0 = 6000$ K (Fig. 7a) and $T_0 = 4000$ K (Fig. 7b). The moment of quenching is clearly visible in both figures at a time ~ 0.1 s for practically any compound. Both versions demonstrate common trends in the development of chemical transformations in hot expanding vapor, despite the fact that concentrations of the quenched compounds may vary considerably at different initial temperatures. In what follows, we analyze the version for $T_0 = 6000$ K.

By the time $t \sim 1$ s, when the size of the cloud grows to a value on the order of $d_{\rm c,\,v} \sim 300$ m (the vapor density $\rho_{\rm v} \sim 10^{-9}$ g cm^{-3} in the vapor cloud at this moment becomes approximately equal to the density of the gaseous coma that surrounds the nucleus; hence, it is necessary to take into account its effect on the expansion of the cloud at later times), its temperature is $T_{\rm v} \sim 600$ K, and composition of the shock-evaporated material manifests the following specifics of behavior. The main hydrogen-containing compounds are: molecular hydrogen H_2 (the fraction $[H_2]$ $\delta_{H_2} \simeq 30\%$ is normalized to the total concentration of hydrogen atoms), atomic hydrogen H ($\delta_{\rm H} \simeq 10\%$), and water H_2O ($\delta_{H_2O} \simeq 15\%$). Carbon is mostly bound into carbon oxide

[5] The presence of dust in the hot expanding gas may result in this gas becoming thermodynamically equilibrium at considerably lower temperatures as well.

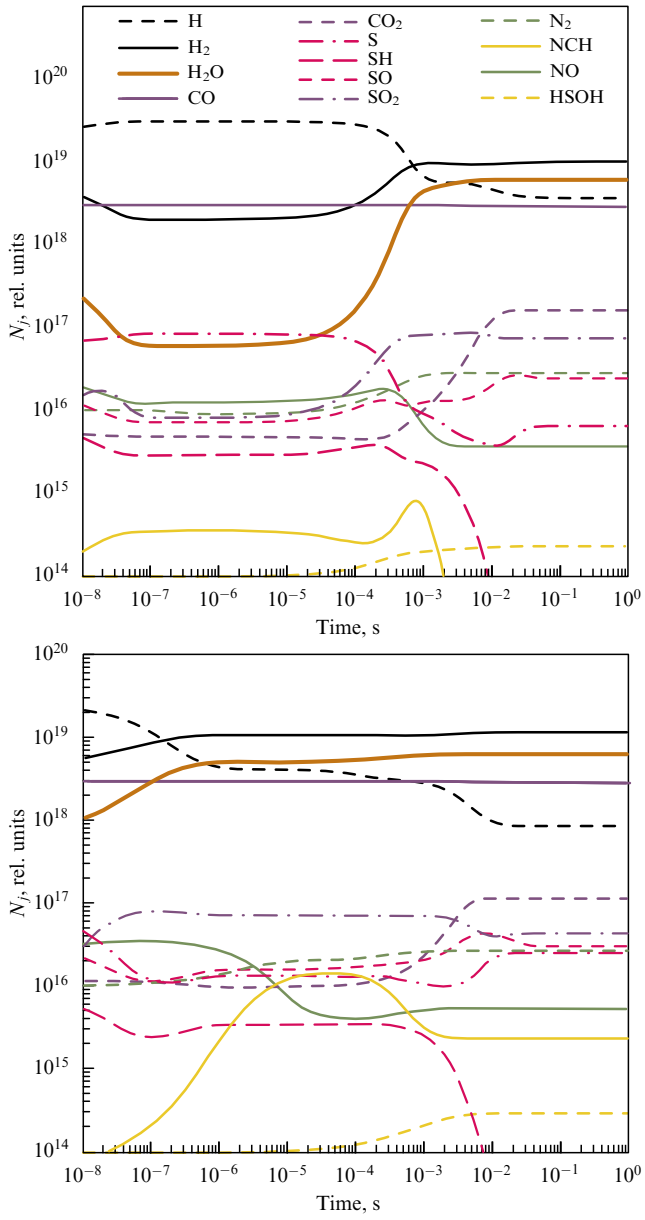

Figure 7. Photochemistry of the inertially expanding hot cloud with a fixed elemental composition (H:O:C:N:S = 60:30:10:1:0.3). The initial gas density: $\rho_0 \simeq 10^{-3}$ g cm^{-3}, the initial gas temperature: $T_0 = 6000$ K (a) and $T_0 = 4000$ K (b). The figures show concentrations of the most important compounds (from the standpoint of observations) of hydrogen, oxygen, carbon, nitrogen, and sulfur.

CO ($\delta_{CO} \simeq 99\%$), the fraction of carbon dioxide CO_2 coming to less than 1%. The main oxygen-containing compounds are atomic oxygen O ($\delta_O \simeq 48\%$), CO ($\delta_{CO} \simeq 32\%$), O_2 ($\delta_{O_2} \simeq 8\%$), H_2O ($\delta_{H_2O} \simeq 2.5\%$), and SO_2 ($\delta_{SO_2} \simeq 1\%$). Nitrogen is mostly converted to molecular nitrogen N_2 ($\delta_{N_2} \simeq 45\%$) and nitrogen oxide NO ($\delta_{NO} \simeq 10\%$). Sulfur-containing compounds present in the vapor are represented by sulfur dioxide SO_2 ($\delta_{SO_2} \simeq 88\%$), sulfur oxide SO ($\delta_{SO} \simeq 9\%$), sulfur S ($\delta_S \simeq 2\%$), HSOH ($\delta_{HSOH} \simeq 0.5\%$), and H_2SO ($\delta_{H_2SO} \simeq 0.3\%$).

Many of the compounds discussed, such as OH, NO, CO, SO, H_2O, CO_2, and SO_2 are efficient emitters at post-collision temperatures, which may support optical depth in the shock-evaporated cometary material in the visible, UV, and IR ranges. In this case, the collision of the impactor and comet nucleus in the Deep Impact experiments should be accompanied by a flash of emitted radiation. Simple arguments serve to evaluate how the spectral intensity of radiation I_λ of the vapor cloud depends on time t,

$$I_\lambda \sim \pi d_{cl}^2 \exp\left(-\frac{E_\lambda}{T_v}\right) \propto t^2 \exp\left[-\alpha_\lambda t^{3(\gamma-1)}\right], \qquad (7)$$

where γ is the adiabat exponent in hot gas, E_λ is the characteristic transition energy in the emitting atom or molecule, λ is the wavelength, T_v is the temperature of the shock vapor, and α_λ is a numerical coefficient.

The first factor describes how the area of the emitter (hot cloud) increases in the process of inertial expansion ($d_{cl} \sim c_{s,cl} t$) provided this cloud is optically thick at the given wavelength. The second factor describes the distribution of concentration and of emitting molecules in the Boltzmann approximation, as functions of gas temperature, without specifying what the molecules are. The changing temperature in the cloud in the process of expansion is taken into account. At the late stages of expansion the shock-evaporated cometary material of the cloud is optically thin and thus turns into a bulk emitter. The function $I_\lambda(t)$ now changes to

$$I_\lambda \propto \exp(-A_\lambda t), \qquad (8)$$

where we included the quenching of the emitting compounds. The exponential factor reflects the drop in the concentration n_j of emitting molecules in the absence of pumping: $dn_j/dt = -A_\lambda n_j$, where A_λ^{-1} is the radiation lifetime of an emitting atom or molecule. The above expression describes the afterglow stage of the cloud as it cools down; the characteristic time of this afterglow is determined by the values of A_λ and may vary in a broad range: from a fraction of a second to several hours. From the observational point of view, of interest are those transitions for which the radiation lifetime is not too large and coincides within an order of magnitude with the time of expansion of the hot cloud (in our case this is a time on the order of several seconds) during which the cloud of cometary vapor still remains an efficient emitter.

For instance, IR radiation is generated as a result of such transitions from metastable levels in vibrationally excited molecules of NO (radiation wavelength $\lambda \simeq 5.3$ μm), CO ($\lambda \simeq 4.6$ μm), OH ($\lambda \simeq 2.8$ μm), and CO_2 ($\lambda \sim 4.3-15$ μm). Transitions from excited rotational levels result in radio admission. Note the line $\lambda = 18$ cm in the hydroxyl molecule OH, which can be detected by ground-based radio telescopes, and the maser radiation of water molecules near the transition 557 GHz, which is generated as a result of rapid expansion and then cooling of cometary ejecta. Radio observation of the above molecules may provide important information on the velocity of expansion of the cloud and, correspondingly, the initial temperature of the shock-evaporated cometary material.

It is necessary to remark here that the above data on the composition of shock-evaporated matter are to a degree tentative and rather reflect the type of tendencies in chemical transformations which depend in a complicated manner on the composition of the cometary material, for instance on the ratio [O]/[C], the mass ratio of the dust and gas components in the cometary nucleus and a number of other factors. The

possibility of detonation of the comet nucleus induced by the impact must not be ruled out either, although realization of this scenario requires a very special chemical composition of the comet matter and optimized impact parameters.

For example, we were in fact using above the data on the observed composition of the coma for the elemental composition of the shock vapor. If, however, the elemental composition of the cometary nucleus is based on the elemental composition of the Sun (the basic element in this case is hydrogen [23]; $[H] \simeq 0.99$, $[O] \simeq 7.4 \times 10^{-4}$, $[O]/[C] \simeq 1.7$, $[O]/[N] \simeq 8$, $[O]/[S] \simeq 40$), then the main quenched compounds of the evaporated material are, according to our kinetic calculations: hydrogen-containing compounds H, H_2; oxygen-containing compounds H_2O, CO; carbon-containing compounds CO; nitrogen-containing compounds N_2, N, HCN, NO; sulfur-containing compounds S, SO. Nevertheless, the chemical composition of the shock-evaporated cometary material and the dynamics of its variation with time (these can be determined from the radiation emitted by the hot cloud) are important factors in determining the initial chemical composition of the shock vapor and, correspondingly, of the chemical composition of volatile compounds in the cometary nucleus. Taking into account that the characteristic time of formation of hot vapor under impact is approximately 0.3 ms, while the penetration depth of both the impactor and a strong shock wave does not exceed 2 m, we can conclude that the vapor composition above should be representative of the composition of the modified surface layer of the cometary nucleus.

6. Conclusions

We have discussed in this paper a number of possible observable effects that accompany a hypervelocity collision between the impactor and the nucleus of the comet Tempel 1 in the Deep Impact active space experiment. We list below the observable consequences of the impact that we regard as most important:

• the impact produces a crater whose size depends on the density and porosity of the comet's nucleus: in the case of non-porous ice the crater diameter is about 80 m, in the case of porous ice of $Po \simeq 0.5$ the crater is smaller by about an order of magnitude, $\simeq 7$ m. In both cases the craters are observable to instruments on board the space probe Deep Impact. The crater size will therefore allow an indirect evaluation of the density and porosity of the cometary nucleus;

• in the case of vertical impact, the unloading in the shock-compressed cometary material generates a cloud of hot vapor, whose composition coincides with the composition of volatile compounds in the surface layer of the cometary nucleus; the cloud temperature increases significantly with increasing porosity of comet's nucleus. The characteristic initial temperature of shock vapor is $T_0 \sim 5000$ K for non-porous ice and $T_0 \sim 15{,}000$ K for porous ice of $Po \simeq 0.5$ porosity. This will be another way of indirectly evaluating the density and porosity of the target;

• as the shock vapor expands, its chemical composition undergoes strong modifications followed by quenching. The main quenched compounds of the shock vapor of the model-composition cometary nucleus are atomic hydrogen and oxygen H, O, molecular oxygen and nitrogen O_2, N_2, hydroxyl OH, water vapor H_2O, carbon oxide and dioxide CO, CO_2, nitrogen oxide NO, sulfur dioxide and oxide SO_2, SO, and the compounds HSOH and H_2SO. Light emission from these compounds will generate a flash in the visible optical, UV, IR, and radio bands that can be detected both on board the Deep Impact probe and by telescopes from Earth.

More than 17 observatories in many countries, as well as the Hubble Space Telescope and a number of instruments in space, will conduct observations of the Deep Impact active experiment. We hope that the results given here may prove useful for the interpretation of the observational data expected in the nearest future.

Acknowledgments

This study was supported by Presidium RAS programs: ''Thermophysics and Mechanics of Intensive Energetic Impacts'' and ''Numerical Simulations'', by the ''Max Planck Research Awards for International Cooperation (September, 2002)'', subject ''Physics of High Energy Density and Dusty Plasma'', by Russian Federation President's grant ''Scientific School'' No. 1938.2003.2 and by grant of Russian Foundation for Basic Research No. 03-07-90197.

References

1. Safronov V S *Evolyutsiya Doplanetnogo Oblaka i Obrazovanie Zemli i Planet* (Evolution of the Protoplanetary Cloud and Formation of the Earth and the Planets) (Moscow: Nauka, 1969) [Translated into English (Jerusalem: Israel Program for Sci. Translations, 1972)]
2. Sagdeev R Z et al. *Adv. Space Res.* **5** (12) 95 (1985); http://iki.cosmos.ru/ssp/vega.html; http://www.laspace.ru/rus/vega.php
3. Klumov B A et al. *Usp. Fiz. Nauk* **164** 617 (1994) [*Phys. Usp.* **37** 577 (1994)]; Fortov V E et al. *Usp. Fiz. Nauk* **166** 391 (1996) [*Phys. Usp.* **39** 363 (1996)]
4. Asphaug E, Benz W *Icarus* **121** 225 (1996)
5. Weissman P R *Nature* **320** 242 (1986); Weidenschilling S J *Nature* **368** 721 (1994)
6. http://stardust.jpl.nasa.gov/photo/cometwild2.html
7. Berezhnoi A A, Klumov B A *Pis'ma Zh. Eksp. Teor. Fiz.* **68** 150 (1998) [*JETP Lett.* **68** 163 (1998)]; Klumov B A, Berezhnoi A A *Adv. Space Res.* **30** 1875 (2002)
8. A'Hearn M F, Belton M J S, Delamere A, Blume W H "Deep Impact: a large-scale active experiment on a cometary nucleus" *Space Sci. Rev.* (2005) (in press)
9. http://deepimpact.jpl.nasa.gov/tech/instruments.html
10. Fernández Y R et al. *Icarus* **164** 481 (2003)
11. Binzel R P et al. *Planet. Space Sci.* **51** 443 (2003)
12. Belton M J S, A'Hearn M F *Adv. Space Res.* **24** 1167 (1999)
13. Ishibashi T, Fujiwara A, Fujii N *Jpn. J. Appl. Phys.* **29** 2543 (1990)
14. Kadono T *Planet. Space Sci.* **47** 305 (1999)
15. Ahrens T J, O'Keefe J D *Int. J. Impact Eng.* **5** 13 (1987)
16. Toon O B et al. *Rev. Geophys.* **35** 41 (1997)
17. Artemieva N A, Shuvalov V V *Deep Sea Res. Pt. II* **49** 959 (2002)
18. Bushman A V, Kanel' G I, Ni A L, Fortov V E *Teplofizika i Dinamika Intensivnykh Impul'snykh Vozdeistvii* (Thermophysics and Dynamics of Pulse Power) (Chernogolovka: OIKhF AN SSSR, 1988)
19. Fortov V E et al. *Nucl. Sci. Eng.* **123** 169 (1996)
20. Cottin H, Gazeau M C, Raulin F *Planet. Space Sci.* **47** 1141 (1999)
21. Zeldovich Ya B, Raizer Yu P *Fizika Udarnykh Voln i Vysokotemperaturnykh Gidrodinamicheskikh Yavlenii* (Physics of Shock Waves and High-Temperature Hydrodynamic Phenomena) (Moscow: Nauka, 1963) [Translated into English (New York: Academic Press, 1966 – 1967)]
22. Berezhnoy A A, Hasebe N, Hiramoto T, Klumov B A *Publ. Astron. Soc. Jpn.* **55** 859 (2003)
23. Anders E, Ebihara M *Geochim. Cosmochim. Acta* **46** 2363 (1982)